Journal of large-scale research facilities

Journal of large-scale research facilities, 4, A129 (2018) http://dx.doi.org/10.17815/jlsrf-4-110

Published: 19.03.2018

E2: The Flat-Cone Diffractometer at BER II

Helmholtz-Zentrum Berlin für Materialien und Energie [*]

Instrument Scientists:
- Dr. J.-U. Hoffmann, Helmholtz-Zentrum Berlin für Materialien und Energie, Department Quantum Phenomena in Novel Materials, phone: +49(0)30 8062-42185, e-mail: hoffmann- j@helmholtz-berlin.de
- Dr. M. Reehuis, Helmholtz-Zentrum Berlin für Materialien und Energie, Department Quantum Phenomena in Novel Materials, phone: +49(0)30 8062-42692, e-mail: reehuis@helmholtz-berlin.de

Abstract: The flat-cone diffractometer E2 at the research reactor BER II is a thermal neutron single-crystal diffractometer for 3D reciprocal space mapping by using four delay-line area detectors (300 × 300 mm^2). Alternatively it is suitable for powder measurements with medium resolution and broad 2-theta scattering range.

1 Introduction

The original Flat-Cone Diffractometer, promoted by D. Hohlwein and W. Prandl (Hohlwein et al., 1986) in 1986, had a banana-type detector. With the Next Generation of the Flat-Cone Diffractometer E2 at the research reactor BER II we now provide a thermal neutron single-crystal diffractometer to scan a 3-dimensional part of the reciprocal space in less than five steps by combining the "off-plane Bragg-scattering" and the flat-cone layer concept while using a new computer-controlled tilting axis of the detector bank. Parasitic scattering from cryostat or furnace walls is reduced by an oscillating radial collimator. The datasets and all connected information is stored in one independent NeXus file format for each measurement and can be easily archived. The software package TVneXus deals with the raw data sets, the transformed physical spaces and the usual data analysis tools (e.g. MatLab). TVneXus can convert to various data sets e.g. into powder diffractograms, linear detector projections, rotation crystal pictures or the 2D/3D reciprocal space. For single-crystal work the multi detector bank (four 2D detectors 300 × 300 mm^2) and the sample table can be tilted around an axis perpendicular to the monochromatic beam to investigate upper layers in reciprocal space (Flat-Cone technique). For powder diffraction studies, the multi detector bank sets on only two positions to measure one powder diffrac-

[*]**Cite article as:** Helmholtz-Zentrum Berlin für Materialien und Energie. (2018). E2: The Flat-Cone Diffractometer at BER II . *Journal of large-scale research facilities, 4*, A129. http://dx.doi.org/10.17815/jlsrf-4-110

CC BY

togram covering a scattering range of 80°. On the other hand every detector can be set on an individual position (with gaps between the detectors) for in-situ measurements.

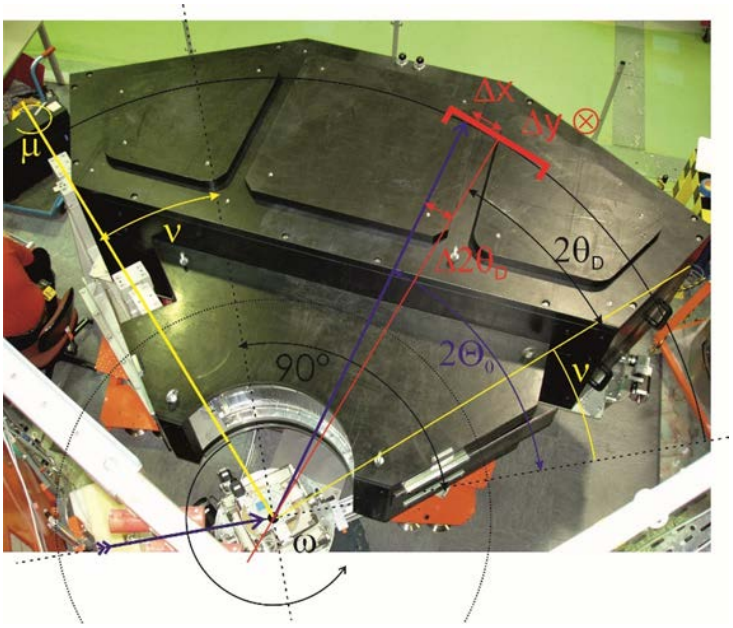

Figure 1: Flat-Cone Diffractometer E2, with the principle geometry axes. (© J.-U. Hoffmann, HZB)

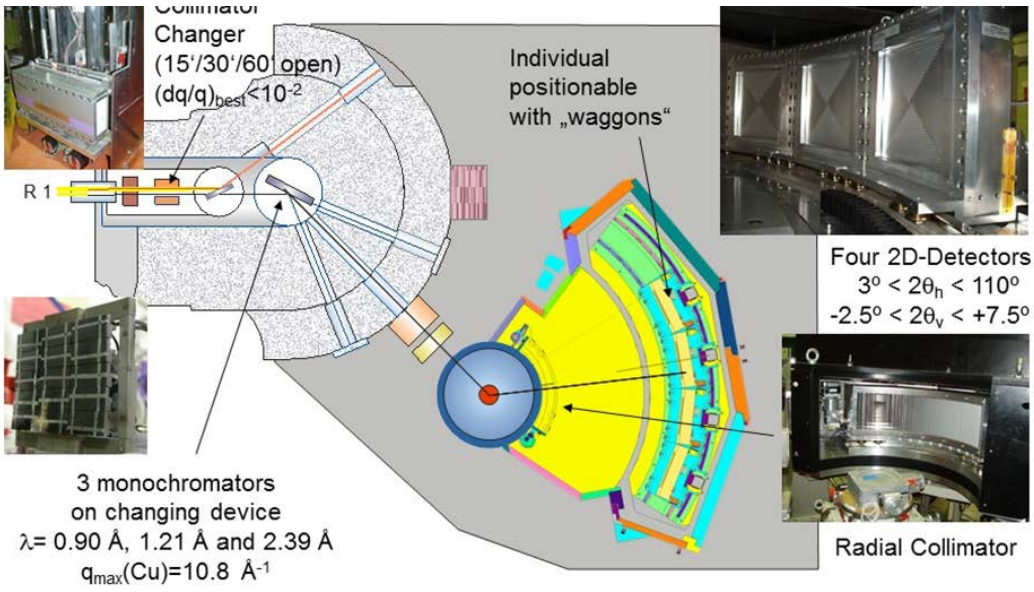

Figure 2: Schematic sketch of E2.

2 Flat-Cone Geometry

The flat-cone technique is a special case of the Weissenberg techniques which were developed earlier in X-ray diffractometry using photographic detectors. In these methods a single crystal rotates around the normal vector of the scattering plane, so that we get a flat disc into the reciprocal-space, recorded along straight lines on a cylindrical film. If only one line is selected by putting a linear aperture in front of the film, then a two-dimensional lattice plane can be mapped on the two-dimensional film by coupling the crystal rotation and the film translation. The same procedure can be realized with a two-dimensional (electronic) multidetector which is placed along one layer line. For each rotational angle of the crystal a separate measurement has to be made. In comparison, earlier used films and linear detector systems have of course a loss in resolution perpendicular to the layer line. On E2 the used two-dimensional detector system can measure a high cylindrical range of the reciprocal space.
The sample table is equipped with a special cradle system which allows a turntable (φ axis) to be tilted by an angle ($0 \leq \mu < 20\,^{\circ}$) around the shaft of the lift up system of the detector bank. The detector with its shielding can be tilted by the same amount around the axis which is perpendicular to the direction of the incident beam in most of our experiments.
An example to calculate upper layer:

With c^* vertical, the layer (h,k,x) can be scanned if one inclines the cradle which is parallel to the beam by an angle μ and the detector by lift up the same angle (μ). The formula in the simplest case is:

$\sin \mu = x \lambda / c$ with $c = 1/c^*$ and the wavelength λ.

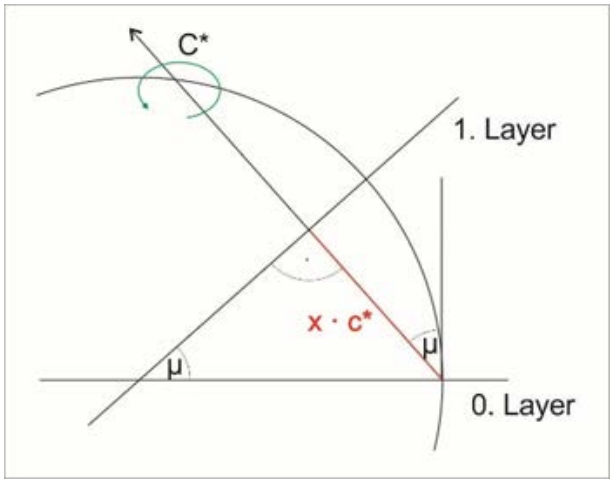

Figure 3: Flat-Cone Geometry in the reciprocal space.

3 Typical Applications

- Representation of complex distributions of superstructure reflections in the reciprocal space using the Flat-Cone technique (Chmielus et al., 2011)
- Determination of commensurate and incommensurate crystal and magnetic structures (Inosov et al., 2009a)
- Diffuse scattering arising from structural and magnetic short-range order (Kaiser et al., 2009)
- Temperature, magnetic and electric field, as well as pressure dependent changes of crystal and magnetic structures (Lottermoser et al., 2004)
- Investigations of structural and magnetic phase transitions
- In-situ kinetics of chemical reactions (Fahr et al., 2001)

CC BY

4 Data analysis and formats

All data sets are stored into the international standard file format Nexus (Könnecke et al., 2015) for easy data exchanges and converting. In order to handle the sample orientations and instrumental geometry a new software package *TVneXus* (Windows 64 Application) was developed to transform collected data into the most useful physical space, e.g. 3D-reciprocal space or powder plots (Intensity over q), and including all necessary corrections such as efficiency of the detector pixels and the integration along Debye-Scherrer cones. The required normalization and merging of data sets are saveable in suitable file formats, e.g. as needed for other evaluation software packages such as *FullProf*. The 3D data sets can variously be stored in form of ASCII, HDF4 or Matlab files, for use with standard visualization and scientific analysis tools. *TVneXus* can work together with the *Matlab* Server. *TVneXus* is able to visualize and analyze one and two-dimensional intensity distributions.

5 Sample Environment

For measurements different sample environments can be used: Temperatures from 30 mK up to 1700 K, vertical magnetic fields up to 6.5 T, horizontal magnetic fields up to 2 T, as well as electric fields and high-pressure. The flat-cone option in combination with a magnet is limited to a vertical magnetic field up to 4.5 T and a maximum tilting angle of $\mu < 11^\circ$

6 Research areas and scientific highlights

6.1 Fast ion conductors and battery materials

Ionic interactions between charge carriers result in complex short-ranged ordered structures, which determine functionality and charging/discharging behavior. Closely related are electrochemical reactions in solid state systems (Kaiser et al., 2009).

6.2 Ferroelectrics

Ferroelectrics are technologically a very important class of materials. The properties of these materials have a close analogy to spin models. Further, new approaches to magnetic systems are applicable (Lottermoser et al., 2004).

6.3 Magneto-caloric materials

A new research focusses on shape memory alloys for room temperature magnetic cooling as well as frustrated and quantum magnets for low temperature effects (Ustinov et al., 2009).

6.4 Novel thermoelectrics

Narrow band frustrated metals theoretically can break the limits on the figure of merit achievable with semiconductors (Roger et al., 2007).

6.5 Multifunctional oxides

Multiferroics, CMR effects, and short range ordering (Hohlwein et al., 2003).

6.6 Intermetallics and heavy Fermion materials

Complex ordering and changes under field and pressure. Influence of site order/disorder effects (Inosov et al., 2009b).

7 Technical Data

Beam tube	R 1B
Collimation	15‘, 30‘, 60‘ (open)
Monochromator	• Cu (220) • Ge (311) • PG (002)
Wave length	• λ = 0.091 nm [Cu (200)] • λ = 0.121 nm [Ge (311)] • λ = 0.241 nm [PG (002)]
Flux	$2 \cdot 10^{-6}$n/cm^{2}s (flat PG monochromator without collimation)
Range of scattering angles	-10° < $2\theta\Theta$ < 107°
Angle resolution	• Horizontal resolution: 0.2° - 0.1° • Vertical resolution: 0.5° - 0.1° • Pixel size 0.1°x0.1°
Detector	Four 2D delay-line detectors (PSD 300 x 300 mm^2)
Tilting angle	0° < μ < 18°
Instrument options	• Single crystal mode • Powder diffraction mode
Software	*TVneXus*

Table 1: Technical parameters of E2.

References

Chmielus, M., Glavatskyy, I., Hoffmann, J.-U., Chernenko, V. A., Schneider, R., & Müllner, P. (2011). Influence of constraints and twinning stress on magnetic field-induced strain of magnetic shape-memory alloys. *Scripta Materialia*, *64*(9), 888 - 891. http://dx.doi.org/10.1016/j.scriptamat.2011.01.025

Fahr, T., Trinks, H. P., Schneider, R., & Fischer, C. (2001). Investigation of the formation of the Bi-2223 phase in multifilamentary Bi-2223/Ag tapes by in situ high temperature neutron diffraction. *IEEE Transactions on Applied Superconductivity*, *11*(1), 3399-3402. http://dx.doi.org/10.1109/77.919792

Hohlwein, D., Hoffmann, J.-U., & Schneider, R. (2003). Magnetic interaction parameters from paramagnetic diffuse neutron scattering in MnO. *Phys. Rev. B*, *68*, 140408. http://dx.doi.org/10.1103/PhysRevB.68.140408

Hohlwein, D., Hoser, A., & Prandl, W. (1986). Collection of Bragg data with a neutron flat-cone diffractometer. *Journal of Applied Crystallography*, *19*(4), 262–266. http://dx.doi.org/10.1107/S002188988608946X

Inosov, D. S., Evtushinsky, D. V., Koitzsch, A., Zabolotnyy, V. B., Borisenko, S. V., Kordyuk, A. A., … Büchner, B. (2009a). Electronic Structure and Nesting-Driven Enhancement of the RKKY Interaction at the Magnetic Ordering Propagation Vector in Gd_2PdSi_3 and Tb_2PdSi_3. *Phys. Rev. Lett.*, *102*, 046401. http://dx.doi.org/10.1103/PhysRevLett.102.046401

Inosov, D. S., Evtushinsky, D. V., Koitzsch, A., Zabolotnyy, V. B., Borisenko, S. V., Kordyuk, A. A., … Büchner, B. (2009b). Electronic Structure and Nesting-Driven Enhancement of the RKKY Interaction

CC BY

at the Magnetic Ordering Propagation Vector in Gd_2PdSi_3 and Tb_2PdSi_3. *Phys. Rev. Lett.*, *102*, 046401. http://dx.doi.org/10.1103/PhysRevLett.102.046401

Kaiser, I., Boysen, H., Frey, F., Lerch, M., Hohlwein, D., & Schneider, R. (2009). Diffuse scattering in quaternary single crystals in the system Zr-Y-O-N. *Zeitschrift für Kristallographie - Crystalline Materials*, *215*(8), 437–440. http://dx.doi.org/10.1524/zkri.2000.215.8.437

Könnecke, M., Akeroyd, F. A., Bernstein, H. J., Brewster, A. S., Campbell, S. I., Clausen, B., … Wuttke, J. (2015). The NeXus data format. *Journal of Applied Crystallography*, *48*(1), 301–305. http://dx.doi.org/10.1107/S1600576714027575

Lottermoser, T., Lonkai, T., Amann, U., Hohlwein, D., Ihringer, J., & Fiebig, M. (2004). Magnetic phase control by an electric field. *Nature*, *430*(6999), 541–544. http://dx.doi.org/10.1038/nature02728

Morris, D. J. P., Tennant, D. A., Grigera, S. A., Klemke, B., Castelnovo, C., Moessner, R., … Perry, R. S. (2009). Dirac Strings and Magnetic Monopoles in the Spin Ice $Dy_2Ti_2O_7$. *Science*, *326*(5951), 411–414. http://dx.doi.org/10.1126/science.1178868

Roger, M., Morris, D. J. P., Tennant, D. A., Gutmann, M. J., Goff, J. P., Hoffmann, J. U., … Deen, P. P. (2007). Patterning of sodium ions and the control of electrons in sodium cobaltate. *Nature*, *445*(7128), 631–634. http://dx.doi.org/10.1038/nature05531

Ustinov, A., Olikhovska, L., Glavatska, N., & Glavatskyy, I. (2009). Diffraction features due to ordered distribution of twin boundaries in orthorhombic Ni–Mn–Ga crystals. *Journal of Applied Crystallography*, *42*(2), 211–216. http://dx.doi.org/10.1107/S0021889809007171